Pharmacokinetics of Long-Acting Tenofovir Alafenamide (GS-7340) Subdermal Implant for HIV Prophylaxis

Manjula Gunawardana,[a] Mariana Remedios-Chan,[b] Christine S. Miller,[a] Rob Fanter,[a] Flora Yang,[a] Mark A. Marzinke,[c,d] Craig W. Hendrix,[c] Martin Beliveau,[e] John A. Moss,[a] Thomas J. Smith,[a,b] Marc M. Baum[a]

Department of Chemistry, Oak Crest Institute of Science, Monrovia, California, USA[a]; Auritec Pharmaceuticals, Inc., Pasadena, California, USA[b]; Department of Medicine, Johns Hopkins University, Baltimore, Maryland, USA[c]; Department of Pathology, Johns Hopkins University, Baltimore, Maryland, USA[d]; Pharsight Consulting Services, Montreal, Quebec, Canada[e]

Oral or topical daily administration of antiretroviral (ARV) drugs to HIV-1-negative individuals in vulnerable populations is a promising strategy for HIV-1 prevention. Adherence to the dosing regimen has emerged as a critical factor determining efficacy outcomes of clinical trials. Because adherence to therapy is inversely related to the dosing period, sustained release or long-acting ARV formulations hold significant promise for increasing the effectiveness of HIV-1 preexposure prophylaxis (PrEP) by reducing dosing frequency. A novel, subdermal implant delivering the potent prodrug tenofovir alafenamide (TAF) with controlled, sustained, zero-order (linear) release characteristics is described. A candidate device delivering TAF at 0.92 mg day^{-1} *in vitro* was evaluated in beagle dogs over 40 days for pharmacokinetics and preliminary safety. No adverse events related to treatment with the test article were noted during the course of the study, and no significant, unusual abnormalities were observed. The implant maintained a low systemic exposure to TAF (median, 0.85 ng ml^{-1}; interquartile range [IQR], 0.60 to 1.50 ng ml^{-1}) and tenofovir (TFV; median, 15.0 ng ml^{-1}; IQR, 8.8 to 23.3 ng ml^{-1}), the product of *in vivo* TAF hydrolysis. High concentrations (median, 512 fmol/10^6 cells over the first 35 days) of the pharmacologically active metabolite, TFV diphosphate, were observed in peripheral blood mononuclear cells at levels over 30 times higher than those associated with HIV-1 PrEP efficacy in humans. Our report on the first sustained-release nucleoside reverse transcriptase inhibitor (NRTI) for systemic delivery demonstrates a successful proof of principle and holds significant promise as a candidate for HIV-1 prophylaxis in vulnerable populations.

Oral or topical daily administration of antiretroviral (ARV) drugs to HIV-1-negative individuals in vulnerable populations is a promising strategy for HIV-1 prevention, but clinical outcomes have varied widely (1–3). Adherence to frequent dosing is burdensome to the user and has emerged as a key factor in explaining the heterogeneous efficacy outcomes of HIV-1 preexposure prophylaxis (PrEP) clinical trials (4–7). It is well established across different delivery methods that adherence to therapy is inversely related with the dosing period (8–11). Sustained-release or long-acting ARV formulations hold significant promise as a means of reducing dosing frequency, thereby increasing the effectiveness of HIV-1 PrEP.

Long-acting preexposure prophylaxis (LA-PrEP) is an alternative regimen to daily dosing designed to mitigate the above-described adherence challenges (12, 13). LA-PrEP has been based primarily on ARV nanoparticles for parenteral administration as injections (12, 14). Dosing intervals of 1 month or longer for injectable, long-acting, nanomilled formulations of the integrase strand-transfer inhibitor cabotegravir (GSK1265744) and the nonnucleoside reverse transcriptase inhibitor (NNRTI) rilpivirine are undergoing clinical evaluation as possible regimens for HIV-1 therapy and prevention (12, 13, 15). While these efforts are encouraging, they do not take advantage of the full portfolio of ARV agents currently available, especially drugs from the established nucleoside reverse transcriptase inhibitor (NRTI) mechanistic class.

Five recent clinical trials have demonstrated that vaginal and oral preparations of the NRTI tenofovir (TFV) can be effective in HIV-1 PrEP (16–20). Therefore, a sustained-release TFV is a logical and highly desirable addition to the small group of LA-PrEP candidates. Unfortunately, established ARV formulation approaches are not amenable to developing a long-acting TFV formulation. The dosing frequency of long-acting ARV agents is determined by the drug's aqueous solubility, antiviral potency, and systemic clearance kinetics. These criteria severely limit the number of FDA-approved ARV agents suitable for reformulation as nanoparticles (12). The high aqueous solubilities (>5 mg ml^{-1}) of TFV, as well as its prodrugs TFV disoproxil fumarate (TDF) and TFV alafenamide (TAF; GS-7340), make long-acting nanoformulations unfeasible.

We have recently reported on a novel approach to achieve parenteral sustained-release ARV delivery based on large (>50 μm), monodisperse drug particles coated with biocompatible polymers that control the compound's release kinetics (21) and have used it to develop long-acting injectable formulations of the NNRTI nevirapine (LA-NVP). Pharmacokinetic (PK) modeling showed that LA-NVP holds promise as a prophylactic in mother-to-child transmission of HIV-1, providing 6 weeks of protective plasma drug levels in the HIV-1-negative infant from a single subcutane-

ous injection at birth (21). Unfortunately, preliminary studies using large TAF crystals coated with the blocking polymer poly(D,L-lactic acid) did not sufficiently slow the *in vitro* release rate for a viable sustained-release candidate in HIV-1 PrEP, where a dosing interval of 1 month or longer typically is required. Therefore, alternative, novel sustained-release drug delivery technologies are required to broaden the number of available agents for HIV-1 LA-PrEP.

A long-acting TFV formulation must overcome the drug's low potency and high aqueous solubility while taking advantage of its slow systemic clearance kinetics. To demonstrate antiviral activity against HIV-1, TFV must undergo *in vivo* phosphorylation to the active moiety, TFV diphosphate (TFV-DP), in cells supporting HIV-1 replication (22). Because TFV-DP is ionized and trapped intracellularly, it persists with a longer half-life than the parent drug in plasma (22). The intracellular half-life of TFV-DP in peripheral blood mononuclear cells (PBMCs) of healthy individuals was estimated at 48 h (23). The prodrug TAF (50% effective concentration [EC_{50}], 5 nM) is 1,000 times more potent than TFV and 10 times more potent than the prodrug TDF (24), making TAF the logical choice as the TFV moiety in the development of a long-acting formulation. Oral TAF also leads to lower plasma TFV exposure than oral TDF (25), a favorable characteristic for long-term safety.

Subdermal implants constitute another means of achieving sustained, controlled release of drugs, but this route has received little attention for the delivery of ARV agents. Chen et al. developed NVP implants that maintained steady-state plasma levels in rats for 90 days (26). An intravitreal implant delivering the antiviral drug ganciclovir for 8 months was developed for the treatment of cytomegalovirus retinitis in AIDS patients (27, 28). Here, a novel subdermal implant for sustained-release TAF is described. The geometry and size of the device is based on widely used contraceptive implants. The prototype device was evaluated for PKs and preliminary safety in beagle dogs over 40 days. Sustained TFV-DP levels in PBMCs significantly exceeded those believed to be required for efficacious HIV-1 PrEP.

MATERIALS AND METHODS

Materials. Tenofovir alafenamide (TAF) was kindly provided by Gilead Sciences, Inc. (Foster City, CA), under a material transfer agreement (MTA) dated 8 November 2013. Polyvinyl alcohol (PVA) with a mean molecular weight (M_w) of 85,000 to 124,000 (98 to 99% hydrolyzed) was obtained from Sigma-Aldrich (St. Louis, MO). Tenofovir-[adenine-$^{13}C_5$] (TFV-$^{13}C_5$) was obtained from Moravek Biochemicals, Inc. (Brea, CA), and maraviroc-D_6 (MVC-D_6) was obtained from Santa Cruz Biotechnology, Inc. (Dallas, TX). All other reagents were obtained from Sigma-Aldrich unless otherwise noted.

Formulation of TAF long-acting (TAF LA) subdermal implant. Sections (40 mm long) of medical-grade platinum cured silicone tubing (721048; 1.5 mm inner diameter [ID] and 1.9 mm outer diameter [OD]; Harvard Apparatus, Holliston, MA) were plasma etched using a model PDC-32G plasma cleaner (Harrick Plasma, Ithaca, NY) at a medium radio frequency (RF) setting for 3 min. Fourteen delivery channels (1.0 mm diameter) per implant were mechanically punched (Fig. 1) as described previously (29). Both open ends were sealed using silicone adhesive (MED3-4213; NuSil Technology LLC, Carpinteria, CA). The sealed segments were dip coated in 5% (wt/wt) PVA solution, air dried overnight at room temperature (25°C), and dip coated a second time with 10% (wt/wt) PVA solution, followed by another round of drying. The silicone plug at one end of the segments was removed and a metal pin inserted, followed by thermal processing at 190°C for 4.75 h (27) and removal of the pin. The
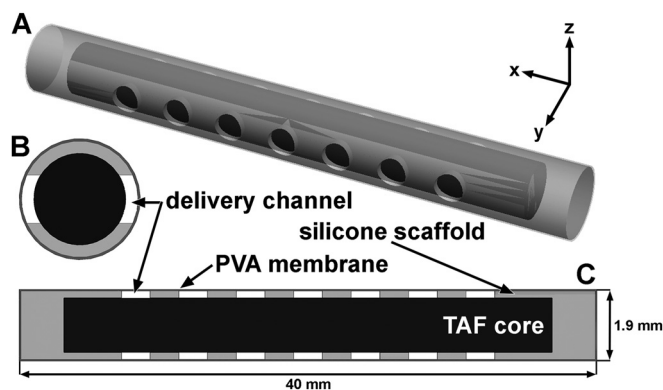

FIG 1 Three-dimensional model (A) and cross-sectional drawings (B and C) of TAF implant. The TAF core (black) inside the silicone scaffold with PVA membrane coating is shown (not to scale). Cross sections were sliced through the *y-z* (B) and *x-y* planes (C).

resulting devices were packed with pure TAF powder without the use of excipients, and the open end was resealed with silicone adhesive. The implants were dried overnight at room temperature, and the exterior was cleaned with an applicator wetted with 1× phosphate-buffered saline solution (PBS; Thermo Fisher Scientific, Inc., Hudson, NH). PVA membrane thickness was determined for implants sectioned in the *y-z* plane (Fig. 1B) using methods described previously (30).

***In vitro* release kinetics measurements.** *In vitro* release studies were designed to mimic sink conditions and were carried out as follows. The implants were placed in dissolution medium (100 ml) consisting of 1× PBS with 0.01% NaN_3 added to prevent microbial growth. The vessels were agitated in an orbital shaker at 25 ± 2°C and 72 rpm. Aliquots (150 μl) were removed at predetermined time points and analyzed by UV absorption spectroscopy (λ_{max} = 262 nm) using a SpectraMax plus absorbance microplate reader (Molecular Devices, Sunnyvale, CA) to determine the TAF concentration using a ten-point standard curve.

Animals. The PK and preliminary safety animal study was carried out at MPI Research, Inc. (Mattawan, MI). Animals were handled in strict accordance with the *Guide for the Care and Use of Laboratory Animals* (31) under approved internal Institutional Animal Care and Use Committee protocols using MPI Research standard operating procedures. Male beagle dogs (*Canis lupus familiaris*; n = 4) between the ages of ca. 13 and 19 months were used in the study. Animals were housed under standard conditions, had *ad libitum* access to water and a standard laboratory diet, and were between 9.2 and 12.4 kg at the time of implantation.

Implantation procedure. The animals were fasted overnight prior to implantation and through at least 1 h postimplantation. The anesthetized animal was placed in ventral recumbency on the surgical table and prepped for sterile surgery using chlorhexidine scrub and solution. A running medial lateral skin incision (1 cm) was made, 2 cm to the side of the vertebral column in the dorsal scapular region. Within the incision line, a subcutaneous pocket (ca. 5 cm by 2 cm) was made by blunt dissection for placement of the TAF LA implant using a hemostat or forceps to pull the implant into the pocket cranial to caudal. Following implantation, the subcutaneous incisions were closed with absorbable sutures and the incisions were closed with staples.

Assessment of toxicity. Toxicity was evaluated by clinical observations, cageside observations (twice daily), and body weight (at least weekly).

Plasma and PBMC sample collection. Blood was collected from the jugular vein at the following predetermined time points postimplantation: 2, 24, 48, 96, 144, 240, 336, 504, 672, 840, and 936 h. Note that whole-blood samples for PBMC isolation and analysis were collected only between 504 and 936 h.

Blood (3 ml) for plasma was collected into tubes containing K_2EDTA as the anticoagulant and maintained on wet ice before being processed for

plasma by centrifugation at 2 to 8°C. Plasma samples were stored and transported frozen at −60 to −90°C.

For PBMC isolation, blood (3 ml) was collected into Vacutainer CPT cell preparation tubes (Becton, Dickinson and Company, Franklin Lakes, NJ) using sodium citrate as the anticoagulant and processed according to the manufacturer's instructions. The layer containing the PBMCs was transferred into a 15-ml tube and brought to a final volume of 14 to 15 ml with $1\times$ Dulbecco's phosphate-buffered saline (DPBS). The suspension was centrifuged at $550 \times g$ for 6 min, the supernatant decanted, and the pellet resuspended in $1\times$ DPBS (final volume of 14 to 15 ml). The suspension was subjected to another round of centrifugation and resuspension of the pellet in $1\times$ DPBS (final volume of 14 to 15 ml). The suspension was centrifuged at $550 \times g$ for 6 min, and the pellet was incubated in red blood cell lysis buffer (5 ml; eBioscience, San Diego, CA) for 5 min at room temperature and protected from light. The mixture was resuspended in $1\times$ DPBS (final volume of 14 to 15 ml) and centrifuged at $550 \times g$ for 6 min. The supernatant was decanted, and the resulting pellet was resuspended in $1\times$ DPBS (1 ml) and transferred into a cryopreservation vial. An aliquot of the suspension was used to count viable PBMCs using a hemocytometer. The number of PBMCs collected per 3-ml whole-blood sample (means ± standard deviations [SD]) was $4.8 \times 10^6 \pm 2.1 \times 10^6$ cells. The remaining suspension was centrifuged at $550 \times g$ for 6 min and the supernatant decanted. The cell pellet was lysed using cold (2 to 8°C) 70% (vol/vol) methanol (0.5 ml), followed by freezing to −50 to −90°C.

Quantification of TAF and TFV plasma concentrations. Dog plasma samples were purified and analyzed separately for TAF and TFV. Plasma samples were thawed on ice, and two 100-μl aliquots were dispensed into separate 96-well plates, along with a minimum of six standards and a minimum of three quality controls, in accordance with FDA guidelines (32). Samples were spiked with 10 μl of internal standard (IS) solution (1 μg ml^{-1} MVC-D$_6$ for TAF and 1 μg ml^{-1} TFV-^{13}C$_5$ for TFV). For TAF, sample purification was carried out in a 96-well format using a protein and phospholipid removal system (Phree; Phenomenex, Inc., Torrance, CA) according to the manufacturer's instructions. For TFV, sample purification was carried out in a 96-well format using a mixed-mode anion exchange and reversed-phase copolymeric sorbent system (Oasis MAX; Waters Corporation, Milford, MA) according to the manufacturer's instructions. The purified samples were dried *in vacuo* using a SpeedVac concentrator system (Savant SC210A Plus; Thermo Fisher Scientific, Inc.) and were reconstituted in 0.1% (vol/vol) formic acid in water (200 μl for TAF, 100 μl for TFV) prior to analysis.

The concentration of TAF was measured at Oak Crest by liquid chromatography-tandem mass spectrometry (LC-MS/MS) using a high-performance liquid chromatography (HPLC) system consisting of a model G1367A well-plate autosampler and a model G1312A binary pump (1200 series; Agilent Technologies, Santa Clara, CA) interfaced to an API 3000 triple-quadrupole tandem mass spectrometer (AB Sciex, Framingham, MA) with a turbo ion spray electrospray ionization (ESI) source. An Agilent Zorbax Eclipse XDB-C$_{18}$ rapid resolution column (2.1×50 mm; 3.5 μm) controlled at 40°C was the stationary phase. The following gradient program was used (A, 0.1%, vol/vol, formic acid in water; B, 0.1%, vol/vol, formic acid in acetonitrile): 0.25 min of 100% A, 0.25-min ramp from 100:0 A:B to 95:5 A:B, 1.5-min ramp from 95:5 A:B to 70:30 A:B, 1.5-min hold at 70:30 A:B, 1.5-min ramp from 70:30 A:B to 95:5 A:B, and 0.5-min ramp from 95:5 A:B to 100:0 A:B. This program resulted in a total run time of 5.5 min with a TAF retention time of 3.5 min. The measured transition ions, *m/z*, under ESI+ ionization mode were the following: TAF, 477.0 amu (parent) and 270.0 amu (product); MVC-D$_6$ (IS), 520.7 amu (parent) and 280.6 amu (product).

The concentration of TFV was measured at Oak Crest by LC-MS/MS using the above-described instrumentation and stationary phase. The following gradient program was used (A, 0.1%, vol/vol, formic acid in water; B, 0.1%, vol/vol, formic acid in acetonitrile): 0.25-min ramp from 100:0 A:B to 95:5 A:B, 0.5-min ramp from 95:5 A:B to 100:0 A:B, and 0.25-min

hold at 100:0 A:B. This program resulted in a total run time of 1.0 min, with a TFV retention time of 0.2 min. The measured transition ions, *m/z*, under ESI+ ionization mode were the following: TFV, 288.1 amu (parent) and 176.2 amu (product); TFV-^{13}C$_5$ (IS), 293.1 amu (parent) and 181.2 amu (product).

Both methods used seven-point standard curves (1 to 100 ng ml^{-1} TAF, 10 to 1,000 ng ml^{-1} TFV) prepared in blank plasma and showed linearity in excess of an R^2 value of 0.98. The lower limits of quantification (LLQ) for TAF and TFV in plasma were 0.5 ng ml^{-1} (1 nM) and 5 ng ml^{-1} (17 nM), respectively. Three separately prepared quality-control samples were analyzed at the beginning and end of each sample set to ensure accuracy and precision within 20%, in accordance with FDA bioanalytical validation criteria (32).

Quantification of PBMC TFV-DP concentrations. The concentration of TFV-DP in PBMCs was measured at Johns Hopkins University using established methods (33) that met FDA bioanalytical validation criteria (32). The analytical measuring range of the assay was 50.0 to 1,500 fmol/sample. TFV-DP measurements exceeding the upper limit of quantitation (ULQ) were diluted and reanalyzed. Results were converted to fmol/10^6 cells based on the lysate-specific number of PBMCs present in the sample. Intracellular concentrations were calculated assuming a mean cell volume of 0.2 μl/10^6 PBMCs (34) in order to maintain consistency with prior reports (35).

Used-implant residual drug analysis and *in vivo* release rate. Residual drug in used implants was extracted with 50% (vol/vol) aqueous methanol, and the concentrations of TAF and TFV were measured by high-performance liquid chromatography (HPLC) with UV detection (1100 series; Agilent Technologies). A Phenomenex (Torrance, CA) Atlantis-C$_{18}$ column (2.1 by 100 mm; 5 μm) controlled at 30°C was used as the stationary phase. The following gradient program was used (A, 1.0%, vol/vol, acetic acid and 3.0%, vol/vol, acetonitrile in water; B, acetonitrile): 2 min of 100% A, 2-min ramp from 100:0 A:B to 75:25 A:B, 2-min hold at 75:25 A:B, 2-min ramp from 75:25 A:B to 100:0 A:B, and 3-min hold at 100:0 A:B. The detection wavelength was 260 nm, and the retention times were 9.46 min (TAF) and 1.13 min (TFV). The method run times were 11 min. *In vivo* TAF release rates assumed linear (zero-order) kinetics based on *in vitro* experiments and were calculated by dividing the total amount of drug released (based on residual drug measurements) by the number of days the implants were in place.

Pharmacokinetic data analyses. Noncompartmental analyses (NCA) were performed in Phoenix software (version 6.4; Pharsight Corporation, Sunnyvale, CA) using literature plasma TAF concentration-versus-time plots following oral TAF administration (5 mg kg^{-1}; $F = 8.6\% \pm 0.8\%$) in beagle dogs (35). The NCA was used to determine the volume of distribution (V) and clearance (CL) for use in the simulation.

The systemic parameters determined in the NCA, along with the *in vitro* implant release rates, were used to simulate plasma TAF concentration-versus-time plots in Phoenix software (see Fig. 5). All parameters are defined in the legend to Fig. 5, and the implant dosage form was assumed to have 100% TAF bioavailability.

Statistical analysis. Data set group statistics and plots were carried out using GraphPad Prism (version 6.02; GraphPad Software, Inc., La Jolla, CA). Statistical significance was defined at a P value of <0.05.

RESULTS

Physical characteristics of the TAF LA implant. The physical characteristics of the sustained-release TAF implant are presented in Table 1 and Fig. 1. The orange-brown color of the implant (Table 1) is the result of the dehydration of the PVA backbone during thermal processing, leading to the formation of conjugated double bonds (36, 37). *In vitro* cumulative release profiles (Fig. 2 and Table 1) exhibited burst-free, sustained release with zero-order (linear) kinetics over 30 days.

Residual drug analysis on the used implants showed that, on average, 98% of the TAF payload was delivered over the 40-day

TABLE 1 Physical characteristics of long-acting TAF implant used in the dog study

Physical characteristic	Value for TAF LA implant[a]
Appearance	Orange-brown
Drug loading (mg; means $\pm$ SD)	42.9 $\pm$ 0.3
OD (mm)	1.9
Length (mm)	40
No. of delivery channels	14
Diameter of delivery channels (mm)	1.0
PVA content (%, wt/wt)	7.3
Membrane thickness (μm)	31.2 $\pm$ 3.8
In vitro release rate (mg day^{-1})	0.92 (0.86–0.98)
In vivo release rate (mg day^{-1})	1.07 (1.04–1.10)

[a] Data in parentheses are the 95% confidence intervals.

study: residual TAF, 0.85 $\pm$ 0.81 mg (means $\pm$ SD). Only traces of TFV (mean, 0.13 mg) were detectable. The TAF implant *in vitro* dissolution rate (K_d; 0.92 mg day^{-1}) (Table 1) was not statistically significantly different ($P = 0.1859$; two-tailed unpaired *t* test with Welch's correction) from the *in vivo* release rate (K_a; 1.07 mg day^{-1}) (Table 1).

Toxicity. No adverse events related to treatment with the test article were noted during the course of the study. Overall, there were no significant abnormalities, and the majority of clinical observations noted were considered to be incidental, procedure related, or common findings for animals of this species. A lack of appetite was noted on day 3 for all animals and was correlated with minimal/no body weight gain for the majority of the animals through day 21. The loss of appetite appeared to be transient, however, with higher body weights noted for all animals on day 40 compared to body weight values on day −1. The incision sites appeared healthy on days 2 to 9 following surgery, and the staples/ sutures were removed on day 8. There was no clinical evidence of inflammation at the implantation sites and no evidence of toxicity or poor tolerability at the implantation sites throughout the duration of the study. Two animals were placed under veterinary consultation while under study for an open incision site (animal number 102, day 13) and mild erythema in both ears (animal number 104, day 29).
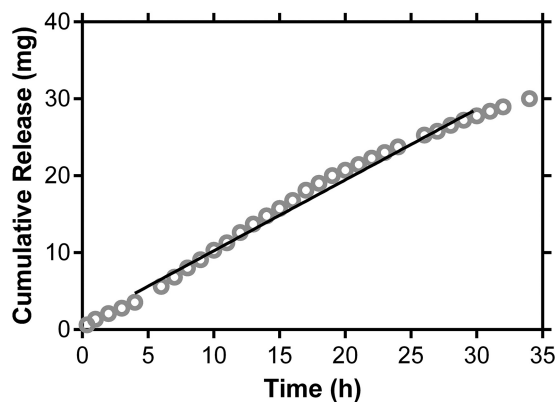

FIG 2 TAF LA displays pseudo-zero-order (linear) cumulative *in vitro* release kinetics (means, $n = 6$). The solid line corresponds to linear regression ($R^2 = 0.8231$) between 4 and 30 days, resulting in a TAF release rate of 0.92 $\pm$ 0.031 mg day^{-1}.
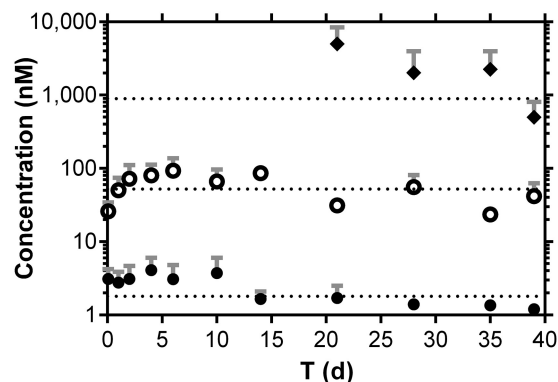

FIG 3 Subdermal implantation of TAF LA prototype device in beagle dogs maintains sustained drug levels with low systemic exposure to TAF and TFV with concomitant, efficient PBMC loading with TFV-DP. Pharmacokinetic profiles of plasma TAF (closed circles) and TFV (open circles) and PBMC TFV-DP (closed diamonds). Each data point represents the means $\pm$ standard deviations from four beagle dogs, and dotted lines correspond to the median concentrations for each analyte over the 40-day study. Note that TFV-DP levels were measured only after day 20.

Pharmacokinetics of sustained-release TAF in dogs. Dog plasma TAF and TFV concentration-versus-time plots following a single subcutaneous dose are shown in Fig. 3, superimposed with TFV-DP PBMC concentrations on days 20 to 40. For TFV-DP measurements below the LLQ but above the limit of detection, the concentration was set to 25 fmol/sample. Only one TFV-DP measurement (day 39) met this criterion (Table 2) and led to a concentration of 32 fmol/10^6 cells (PBMC count for the sample was 3.1 $\times$ 10^6 cells; a 0.25-ml volume was analyzed, resulting in a total of 0.78 $\times$ 10^6 cells analyzed). One measurement exceeded the ULQ (day 21), but there was insufficient sample remaining to dilute and reanalyze, so this sample was omitted from the analysis.

The TAF implants maintained sustained plasma levels of TAF and TFV, as well as PBMC TFV-DP concentrations, for 40 days (Fig. 3). The molar TAF:TFV plasma concentration ratio (median $\pm$ SD, 0.047 $\pm$ 0.024 for days 1 to 40) was stable throughout the study (Fig. 4). These data, along with residual drug analysis, suggest that TAF is stable in the implant for 40 days *in vivo*. The short TAF plasma half-life in dogs (92 min) (35) suggests that if significant prodrug hydrolysis were occurring in the implant, the TAF:TFV plasma concentration ratios would decrease significantly over the course of the study. The

TABLE 2 Summary of TAF, TFV, and TFV-DP concentrations over the course of the 40-day dog study ($n = 4$)

Analyte, matrix[a]	n	% above LLQ[b]	Median (IQR[c])
TAF, plasma	44	100	0.85 (0.60–1.50) ng ml^{-1}; 1.8 (1.3–3.2) nM
TFV, plasma	44	98	15.0 (8.8–23.3) ng ml^{-1}; 52.2 (30.5–81.0) nM
TFV-DP, PBMCs	16	94	179.2[d] (128.2–616.7) fmol/10^6 cells; 895.8 (640.9–3,083) nM

[a] All values correspond to time points with the implant in place.
[b] Proportion of samples that contained quantifiable drug levels.
[c] Interquartile range between the first (25th percentile) and third (75th percentile) quartiles.
[d] Median of 511.8 fmol/10^6 cells (IQR, 165.4 to 735.4 fmol/10^6 cells), over the first 35 days, before TAF release from the implant becomes nonlinear due to drug depletion (Fig. 2).
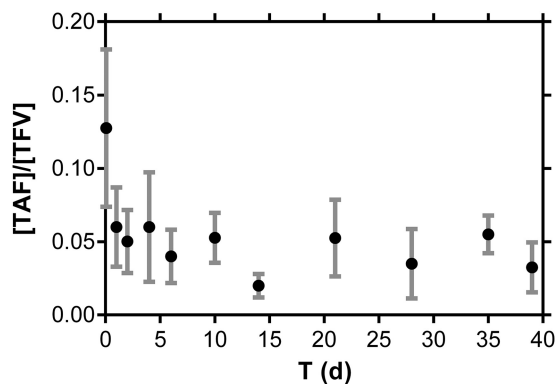
FIG 4 Molar TAF:TFV plasma concentration ratios are stable throughout the 40-day study. Each data point represents the means ± standard deviations from four beagle dogs.

FIG 5 Simulation of TAF pharmacokinetics in beagle dogs based on *in vitro* implant release rates. (A) Graphical model. *C*, simulated plasma TAF concentration; *V*, volume of distribution (6.8 liters); *Cl*, clearance (473 liters day^{-1}); *A0*, amount of drug cleared; *A1*, amount in the central compartment 1; *CObs*, observed plasma TAF concentration; *S1 Rate*, zero-order release rate from implant (1.9 μmol day^{-1}, 0.92 mg day^{-1}). (B) Actual individual (closed circles) and simulated (dotted line) TAF plasma levels. The dose was 90 μmol (43 mg), and the bioavailability (*F*) of the implant was assumed to be 100%. Note the linear *y* axis.

magnitude of the TAF:TFV ratio, i.e., high plasma TFV levels relative to those of TAF in paired samples, suggests that TAF metabolism to TFV could occur *in vivo*, possibly via intracellular dephosphorylation of TFV-DP and transporter-mediated efflux of TFV into blood, in agreement with prior reports (22, 38, 39).

A summary of drug concentrations is presented in Table 2. A median PBMC TFV-DP concentrations of 511.8 fmol/10^6 cells, an underestimate, as the ULQ sample was omitted from the analysis, was observed over the first 35 days, before dipping on day 40 as the implant drug reservoir was being depleted (Fig. 3). A lowering of the daily TAF release rate after 35 days also was observed *in vitro* (Fig. 2), consistent with drug depletion from the implant and as described mechanistically for similar devices in the literature (30).

Simulation of plasma TAF levels. A PK model (Fig. 5A) based on systemic parameters derived by NCA of published data from oral TAF administration in beagle dogs (35) and the measured *in vitro* TAF release rates was used to simulate the corresponding TAF plasma levels *a priori* (Fig. 4B). The purpose of this exercise was not to model the *in vivo* TAF PKs but to predict TAF exposure based purely on *in vitro* release rates and literature PK data. Based on this simple approach, the analysis afforded reasonable agreement between simulated and measured values despite the short TAF plasma half-life in dogs and the low observed concentrations. The lower observed levels after day 30 likely are due to drug depletion from the implant, resulting in a change in release kinetics from zero order to first order (Fig. 2) (30). The model will be refined in the future to take these nonlinear effects into consideration and will be useful in guiding formulation developments.

DISCUSSION

The primary objectives of the current study were to develop a sustained-release TAF implant and to evaluate the PK and preliminary safety of the device in dogs. The results are discussed below with an emphasis on HIV-1 prophylaxis, although it is conceivable that a similar device could be used in the treatment of HIV-1/AIDS.

Pharmacokinetics and preliminary safety of TAF implant prototype in dogs: implications for HIV-1 PrEP. In HIV-1 PrEP, unlike treatment of HIV-1/AIDS, there is no biomarker of ARV drug effect in susceptible, uninfected individuals to guide product development. Randomized clinical trials (RCTs) for PrEP based
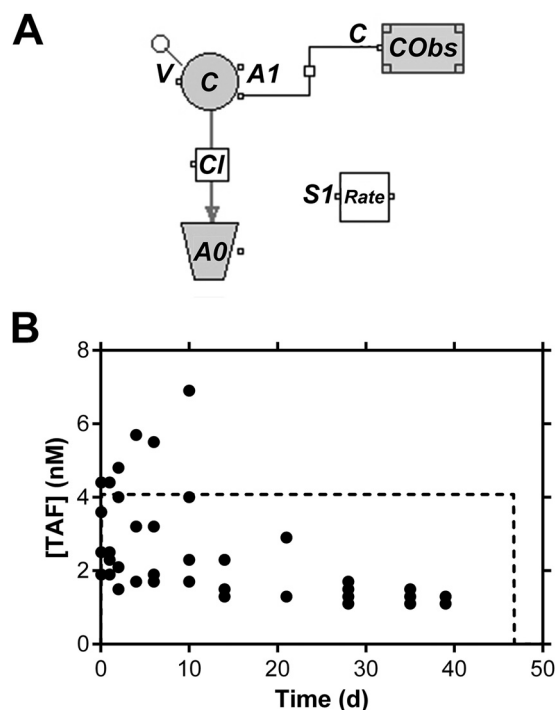
on TFV preparations have used sparse sampling of plasma, PBMCs, or cervicovaginal fluid to correlate measured drug levels (PK) with the primary pharmacodynamic (PD) endpoint: HIV-1 seroconversion. For systemic PrEP, TFV-DP concentration in PBMCs represents an accepted metric for estimating threshold protective drug levels (23, 33, 40–42). In iPrEX, an RCT where HIV-negative men who have sex with men took a daily oral combination of TDF and emtricitabine (FTC), HIV-1 protection was 92% in participants moderately adhering to the regimen, as determined by plasma TFV levels (17). A *post hoc* analysis found that a PBMC TFV-DP concentration of 16 fmol/10^6 cells was associated with 90% protection (43). It should be noted that, unlike in the current study, the iPrEX RCT used cryopreserved PBMCs, which leads to 33 to 67% loss of TFV-DP. Therefore, a more conservative EC$_{90}$ lies in the range of 24 to 48 fmol/10^6 cells. While this tentative prophylactic TFV-DP concentration requires further clinical validation, it represents the best available initial target level in the preclinical development of a TAF implant. Future studies will complement drug measurements in blood by analyzing TFV-DP levels in anatomic compartments believed to be determinants of HIV-1 PrEP efficacy, such as vaginal and rectal tissues and the HIV-1 susceptible immune cells they contain.

In this preliminary study, a subcutaneous implant delivering TAF at a rate of 1.07 ± 0.02 mg day^{-1} for 40 days in beagle dogs maintained median PBMC TFV-DP levels of 512 fmol/10^6 cells over the first 35 days. This achieved median concentration is 11 to 32 times higher than the protective target from iPrEX (corre-

sponding to a TFV-DP concentration range of 16 to 48 fmol/10^6 cells). Simple allometric scaling (44, 45) (exponent, 0.75) from beagle dogs (mean weight, 10.8 kg) to humans (70 kg) affords a preliminary, lower target daily TAF release rate of 0.14 mg day^{-1} to maintain a median TFV-DP PBMC concentration of 16 fmol/10^6 cells. The concentration of PBMCs in beagle dog whole blood (mean, 1.6×10^6 cells/ml; SD, 0.7×10^6 cells/ml) was comparable to typical values for HIV-negative humans. Therefore, a 1-year implant would need to contain at least 51 mg TAF (0.14 mg day^{-1} for 365 days), a feasible quantity for an implant with practical physical dimensions.

Novel implant design for the sustained delivery of water-soluble drugs. A sustained-release formulation of TAF has not been reported. The implant design described here is novel and builds on the success of our pod-intravaginal ring (pod-IVR) system for sustained, highly controlled vaginal drug delivery (29). The implant consists of a drug-filled, PVA-coated silicone cylinder with orthogonal delivery channels (Fig. 1). The number and cross-sectional diameter of the channels, coupled with the physiochemical properties of the outer polymer membrane, determine the implant release rate. The degrees of freedom allow the drug release rate to be tuned over a wide range, even for water-soluble drugs such as NRTIs. The release rate is not influenced by implant drug loading, as in matrix systems where the drug is dispersed in the polymer. The silicone shell is impermeable, and all drug release is through the PVA-coated delivery channels, which linearize drug release. The implant architecture also has the benefit of protecting the drug core from chemical degradation, as evidenced by the *in vivo* stability of the TAF depot over 40 days. Controlled and sustained release is independent of the implant shell material, thereby offering flexibility in polymer choices that may be important for future large-scale production. The successful development of candidates for LA-PrEP in HIV-1 prevention will require devices that are safe, effective, well tolerated, and affordable. The TAF implant prototype described here was designed with these criteria in mind and afforded burst-free, linear TAF release (Fig. 2), a significant advantage over injectable long-acting ARV nanoformulations.

Is a 1-year subdermal TAF implant feasible? The geometry and size of the TAF implant is based on three widely used contraceptive implants. The Norplant subcutaneous contraceptive implant, first approved in 1983 (Finland), consisted of six individual tubular silicone capsules (2.4 mm OD by 34 mm long), each containing 36 mg levonorgestrel (LNG). Approved in 1996, the Norplant II (Jadelle) implant consists of two silicone rods (2.5 mm OD by 43 mm long), each with 75 mg LNG dispersed in the elastomer. The Implanon/Nexplanon devices are single rods (2 mm diameter by 40 mm length) containing 68 mg etonogestrel dispersed in ethylene vinyl acetate (46). These dimensions are identical to those of the prototype TAF implant used in our dog study. All three implant types are inserted subdermally on the inside of the upper arm by making a small incision and using an insertion device consisting of a hollow needle and trochanter for placement. Multiple, individual rods (e.g., Norplant and Jadelle) are implanted in a fan-shaped pattern. The devices also are easily replaced. Insertion/removal of the proposed TAF implants will follow methods identical to those used successfully to insert/remove millions of these contraceptive implants.

Conclusions. A long-acting TAF implant has translational potential as a candidate for HIV-1 prophylaxis in vulnerable populations. Sustained-release TAF delivery could improve drug ad-

herence and reduce transmission compared to levels for daily oral dosing. A TAF implant also holds potential as part of a highly active antiretroviral therapy (HAART) regimen for the treatment of HIV-1/AIDS, especially when combined with other parenteral sustained-release ARV formulations.

REFERENCES

1. Cohen MS, Smith MK, Muessig KE, Hallett TB, Powers KA, Kashuba AD. 2013. Antiretroviral treatment of HIV-1 prevents transmission of HIV-1: where do we go from here? Lancet **382**:1515–1524. http://dx.doi.org/10.1016/S0140-6736(13)61998-4.
2. D'Cruz OJ, Uckun FM. 2014. Vaginal microbicides and their delivery platforms. Expert Opin Drug Deliv **11**:723–740. http://dx.doi.org/10.1517/17425247.2014.888055.
3. McGowan I. 2014. An overview of antiretroviral pre-exposure prophylaxis of HIV infection. Am J Reprod Immunol **71**:624–630. http://dx.doi.org/10.1111/aji.12225.
4. Muchomba FM, Gearing RE, Simoni JM, El-Bassel N. 2012. State of the science of adherence in pre-exposure prophylaxis and microbicide trials. J Acquir Immune Defic Syndr **61**:490–498. http://dx.doi.org/10.1097/QAI.0b013e31826f9962.
5. Amico KR, Mansoor LE, Corneli A, Torjesen K, van der Straten A. 2013. Adherence support approaches in biomedical HIV prevention trials: experiences, insights and future directions from four multisite prevention trials. AIDS Behav **17**:2143–2155. http://dx.doi.org/10.1007/s10461-013-0429-9.
6. Gengiah TN, Moosa A, Naidoo A, Mansoor LE. 2014. Adherence challenges with drugs for pre-exposure prophylaxis to prevent HIV infection. Int J Clin Pharm **36**:70–85. http://dx.doi.org/10.1007/s11096-013-9861-1.
7. Hendrix CW. 2014. Abstr 2014 Conf Retrovir Opportun Infect, abstr 61.
8. Kruse W, Eggertkruse W, Rampmaier J, Runnebaum B, Weber E. 1991. Dosage frequency and drug compliance behavior—a comparative study on compliance with a medication to be taken twice or 4 times daily. Eur J Clin Pharmacol **41**:589–592. http://dx.doi.org/10.1007/BF00314990.
9. Sershen S, West J. 2002. Implantable, polymeric systems for modulated drug delivery. Adv Drug Deliv Rev **54**:1225–1235. http://dx.doi.org/10.1016/S0169-409X(02)00090-X.
10. Kutilek VD, Sheeter DA, Elder JH, Torbett BE. 2003. Is resistance futile? Curr Drug Targets Infect Disord **3**:295–309. http://dx.doi.org/10.2174/1568005033481079.
11. Yeaw J, Benner JS, Walt JG, Sian S, Smith DB. 2009. Comparing adherence and persistence across 6 chronic medication classes. J Manag Care Pharm **15**:728–740.
12. Spreen WR, Margolis DA, Pottage JC. 2013. Long-acting injectable antiretrovirals for HIV treatment and prevention. Curr Opin HIV AIDS **8**:565–571. http://dx.doi.org/10.1097/COH.0000000000000002.
13. Dolgin E. 2014. Long-acting HIV drugs advanced to overcome adherence challenge. Nat Med **20**:323–324. http://dx.doi.org/10.1038/nm0414-323.
14. Williams J, Sayles HR, Meza JL, Sayre P, Sandkovsky U, Gendelman HE, Flexner C, Swindells S. 2013. Long-acting parenteral nanoformulated antiretroviral therapy: interest and attitudes of HIV-infected patients. Nanomedicine **8**:1807–1813. http://dx.doi.org/10.2217/nnm.12.214.
15. Jackson AG, Else LJ, Mesquita PM, Egan D, Back DJ, Karolia Z, Ringner-Nackter L, Higgs CJ, Herold BC, Gazzard BG, Boffito M. 2014. A compartmental pharmacokinetic evaluation of long-acting rilpivirine in HIV negative volunteers for pre-exposure prophylaxis (PrEP). Clin Pharmacol Ther **96**:314–323. http://dx.doi.org/10.1038/clpt.2014.118.
16. Abdool Karim Q, Abdool Karim SS, Frohlich JA, Grobler AC, Baxter C, Mansoor LE, Kharsany ABM, Sibeko S, Mlisana KP, Omar Z, Gengiah TN, Maarschalk S, Arulappan N, Mlotshwa M, Morris L, Taylor D. 2010. Effectiveness and safety of tenofovir gel, an antiretroviral microbicide, for the prevention of HIV infection in women. Science **329**:1168–1174. http://dx.doi.org/10.1126/science.1193748.
17. Grant RM, Lama JR, Anderson PL, McMahan V, Liu AY, Vargas L, Goicochea P, Casapia M, Guanira-Carranza JV, Ramirez-Cardich ME, Montoya-Herrera O, Fernandez T, Veloso VG, Buchbinder SP, Chari-

yalertsak S, Schechter M, Bekker LG, Mayer KH, Kallas EG, Amico KR, Mulligan K, Bushman LR, Hance RJ, Ganoza C, Defechereux P, Postle B, Wang FR, McConnell JJ, Zheng JH, Lee J, Rooney JF, Jaffe HS, Martinez AI, Burns DN, Glidden DV. 2010. Preexposure chemoprophylaxis for HIV prevention in men who have sex with men. N Engl J Med 363:2587–2599. http://dx.doi.org/10.1056/NEJMoa1011205.

18. Baeten JM, Donnell D, Ndase P, Mugo NR, Campbell JD, Wangisi J, Tappero JW, Bukusi EA, Cohen CR, Katabira E, Ronald A, Tumwesigye E, Were E, Fife KH, Kiarie J, Farquhar C, John-Stewart G, Kakia A, Odoyo J, Mucunguzi A, Nakku-Joloba E, Twesigye R, Ngure K, Apaka C, Tamooh H, Gabona F, Mujugira A, Panteleeff D, Thomas KK, Kidoguchi L, Krows M, Revall J, Morrison S, Haugen H, Emmanuel-Ogier M, Ondrejcek L, Coombs RW, Frenkel L, Hendrix C, Bumpus NN, Bangsberg D, Haberer JE, Stevens WS, Lingappa JR, Celum C, Partners PrEP Study Team. 2012. Antiretroviral prophylaxis for HIV prevention in heterosexual men and women. N Engl J Med 367:399–410. http://dx.doi.org/10.1056/NEJMoa1108524.

19. Thigpen MC, Kebaabetswe PM, Paxton LA, Smith DK, Rose CE, Segolodi TM, Henderson FL, Pathak SR, Soud FA, Chillag KL, Mutanhaurwa R, Chirwa LI, Kasonde M, Abebe D, Buliva E, Gvetadze RJ, Johnson S, Sukalac T, Thomas VT, Hart C, Johnson JA, Malotte CK, Hendrix CW, Brooks JT, TDF2 Study Group. 2012. Antiretroviral preexposure prophylaxis for heterosexual HIV transmission in Botswana. N Engl J Med 367:423–434. http://dx.doi.org/10.1056/NEJMoa1110711.

20. Choopanya K, Martin M, Suntharasamai P, Sangkum U, Mock PA, Leethochawalit M, Chiamwongpaet S, Kitisin P, Natrujirote P, Kittimunkong S, Chuachoowong R, Gvetadze RJ, McNicholl JM, Paxton LA, Curlin ME, Hendrix CW, Vanichseni S. 2013. Antiretroviral prophylaxis for HIV infection in injecting drug users in Bangkok, Thailand (the Bangkok tenofovir study): a randomised, double-blind, placebo-controlled phase 3 trial. Lancet 381:2083–2090. http://dx.doi.org/10.1016/S0140-6736(13)61127-7.

21. Cortez JM, Jr, Quintero R, Moss JA, Beliveau M, Smith TJ, Baum MM. 2015. Pharmacokinetics of injectable, long-acting nevirapine for HIV prophylaxis in breastfeeding infants. Antimicrob Agents Chemother 59:59–66. http://dx.doi.org/10.1128/AAC.03906-14.

22. Anderson PL, Kiser JJ, Gardner EM, Rower JE, Meditz A, Grant RM. 2011. Pharmacological considerations for tenofovir and emtricitabine to prevent HIV infection. J Antimicrob Chemother 66:240–250. http://dx.doi.org/10.1093/jac/dkq447.

23. Louissaint NA, Cao YJ, Skipper PL, Liberman RG, Tannenbaum SR, Nimmagadda S, Anderson JR, Everts S, Bakshi R, Fuchs EJ, Hendrix CW. 2013. Single dose pharmacokinetics of oral tenofovir in plasma, peripheral blood mononuclear cells, colonic tissue, and vaginal tissue. AIDS Res Hum Retrovir 29:1443–1450. http://dx.doi.org/10.1089/aid.2013.0044.

24. Lee WA, He GX, Eisenberg E, Cihlar T, Swaminathan S, Mulato A, Cundy KC. 2005. Selective intracellular activation of a novel prodrug of the human immunodeficiency virus reverse transcriptase inhibitor tenofovir leads to preferential distribution and accumulation in lymphatic tissue. Antimicrob Agents Chemother 49:1898–1906. http://dx.doi.org/10.1128/AAC.49.5.1898-1906.2005.

25. Markowitz M, Zolopa A, Squires K, Ruane P, Coakley D, Kearney B, Zhong LJ, Wulfsohn M, Miller MD, Lee WA. 2014. Phase I/II study of the pharmacokinetics, safety and antiretroviral activity of tenofovir alafenamide, a new prodrug of the HIV reverse transcriptase inhibitor tenofovir, in HIV-infected adults. J Antimicrob Chemother 69:1362–1369. http://dx.doi.org/10.1093/jac/dkt532.

26. Chen J, Walters K, Ashton P. 2005. Correlation of in vitro-in vivo release rates for sustained release nevirapine implants in rats. J Control Release 101:357–358.

27. Smith TJ, Pearson PA, Blandford DL, Brown JD, Goins KA, Hollins JL, Schmeisser ET, Glavinos P, Baldwin LB, Ashton P. 1992. Intravitreal sustained-release ganciclovir. Arch Ophthalmol 110:255–258. http://dx.doi.org/10.1001/archopht.1992.01080140111037.

28. Musch DC, Martin DF, Gordon JF, Davis MD, Kuppermann BD, Heinemann MH, Campbell S, Boddice S, Duker JS, Naughton K, McGeary J, Chong LP, Walonker F, Levin L, Lopez K, Gomes A, Davis JL, Simmons T, Vandenbrook R, Fish RH, Hutchison C, Ai E, Luckie A, Tashayyod D, Anand R, Chuang EL, Lawrence B, Robinson MR, Champagne K, Cantrill HL, Brallier A, Freeman WR, Jarman C, Wieland MR, Coverstone V, Ligh JK, Hutt R, Norman BC, Cristiano J, Neger R, Crawford K, Weinberg DV, Munana A, Murphy FP, Pace B, Duh YJ, Gordon JE, Johnson PJ, Lee JA, Pang CF, Safyan E, Seidl NL, Stoecker JF, Ashton P, Smith TJ, Armstrong

J, Brothers R, Hubbard L, Dieterich DT, Frost KR, Maguire MG, Nussenblatt RB, Sanborn GE. 1997. Treatment of cytomegalovirus retinitis with a sustained-release ganciclovir implant. N Engl J Med 337:83–90. http://dx.doi.org/10.1056/NEJM199707103370203.

29. Baum MM, Butkyavichene I, Gilman J, Kennedy S, Kopin E, Malone AM, Nguyen C, Smith TJ, Friend DR, Clark MR, Moss JA. 2012. An intravaginal ring for the simultaneous delivery of multiple drugs. J Pharm Sci 101:2833–2843. http://dx.doi.org/10.1002/jps.23208.

30. Gunawardana M, Baum MM, Smith TJ, Moss JA. 2014. An intravaginal ring for the sustained delivery of antibodies. J Pharm Sci 103:3611–3620. http://dx.doi.org/10.1002/jps.24154.

31. National Research Council. 2001. Guide for the care and use of laboratory animals, 8th ed. The National Academies Press, Washington, DC.

32. U.S. FDA. 2001. Guidance for industry: bioanalytical method validation. U.S. Department of Health and Human Services, Food and Drug Administration, Center for Drug Evaluation and Research (CDER), Center for Veterinary Medicine (CVM), Rockville, MD.

33. Hendrix CW, Chen BA, Guddera V, Hoesley C, Justman J, Nakabiito C, Salata R, Soto-Torres L, Patterson K, Minnis AM, Gandham S, Gomez K, Richardson BA, Bumpus NN. 2013. MTN-001: randomized pharmacokinetic cross-over study comparing tenofovir vaginal gel and oral tablets in vaginal tissue and other compartments. PLoS One 8:e55013. http://dx.doi.org/10.1371/journal.pone.0055013.

34. Chapman EH, Kurec AS, Davey FR. 1981. Cell volumes of normal and malignant mononuclear cells. J Clin Pathol 34:1083–1090. http://dx.doi.org/10.1136/jcp.34.10.1083.

35. Babusis D, Phan TK, Lee WA, Watkins WJ, Ray AS. 2013. Mechanism for effective lymphoid cell and tissue loading following oral administration of nucleotide prodrug GS-7340. Mol Pharm 10:459–466. http://dx.doi.org/10.1021/mp3002045.

36. Byron PR, Dalby RN. 1987. Effects of heat treatment on the permeability of polyvinyl alcohol films to a hydrophilic solute. J Pharm Sci 76:65–67.

37. Petrova NV, Evtushenko AM, Chikhacheva IP, Zubov VP, Kubrakova IV. 2005. Effect of microwave irradiation on the cross-linking of polyvinyl alcohol. Russ J Appl Chem 78:1158–1161. http://dx.doi.org/10.1007/s11167-005-0470-1.

38. Kis O, Robillard K, Chan GNY, Bendayan R. 2010. The complexities of antiretroviral drug-drug interactions: role of ABC and SLC transporters. Trends Pharmacol Sci 31:22–35. http://dx.doi.org/10.1016/j.tips.2009.10.001.

39. Madrasi K, Burns RN, Hendrix CW, Fossler MJ, Chaturvedula A. 2014. Linking the population pharmacokinetics of tenofovir and its metabolites with its cellular uptake and metabolism. CPT Pharmacometrics Syst Pharmacol 12:e147. http://dx.doi.org/10.1038/psp.2014.46.

40. Patterson KB, Prince HA, Kraft E, Jenkins AJ, Shaheen NJ, Rooney JF, Cohen MS, Kashuba ADM. 2011. Penetration of tenofovir and emtricitabine in mucosal tissues: implications for prevention of HIV-1 transmission. Sci Transl Med 3:112re114. http://dx.doi.org/10.1126/scitranslmed.3003174.

41. Hendrix CW. 2013. Exploring concentration response in HIV preexposure prophylaxis to optimize clinical care and trial design. Cell 155:515–518. http://dx.doi.org/10.1016/j.cell.2013.09.030.

42. Trezza CR, Kashuba ADM. 2014. Pharmacokinetics of antiretrovirals in genital secretions and anatomic sites of HIV transmission: implications for HIV prevention. Clin Pharmacokinet 53:611–624. http://dx.doi.org/10.1007/s40262-014-0148-z.

43. Anderson PL, Glidden DV, Liu A, Buchbinder S, Lama JR, Guanira JV, McMahan V, Bushman LR, Casapia M, Montoya-Herrera O, Veloso VG, Mayer KH, Chariyalertsak S, Schechter M, Bekker LG, Kallas EG, Grant RM, iPrEx Study Team. 2012. Emtricitabine-tenofovir concentrations and pre-exposure prophylaxis efficacy in men who have sex with men. Sci Transl Med 4:151ra125. http://dx.doi.org/10.1126/scitranslmed.3004006.

44. West GB, Brown JH. 2005. The origin of allometric scaling laws in biology from genomes to ecosystems: towards a quantitative unifying theory of biological structure and organization. J Exp Biol 208:1575–1592. http://dx.doi.org/10.1242/jeb.01589.

45. Sharma V, McNeill JH. 2009. To scale or not to scale: the principles of dose extrapolation. Br J Pharmacol 157:907–921. http://dx.doi.org/10.1111/j.1476-5381.2009.00267.x.

46. Merck & Co, Inc. 2014. Nexplanon prescribing information. Merck Sharp & Dohme B.V., Whitehouse Station, NJ.